Advanced ultra-high molecular weight polyethylene/antioxidant-functionalized carbon nanotubes nanocomposites with improved thermo-oxidative resistance

Nadka Tzankova Dintcheva,[1] Rossella Arrigo,[1] Cristian Gambarotti,[2] Sabrina Carroccio,[3] Serena Coiai,[4] Giovanni Filippone[5]

[1]Dipartimento di Ingegneria Civile, Ambientale, Aerospaziale, dei Materiali, Università di Palermo, Viale delle Scienze 90128 Palermo, Italy

[2]Dipartimento di Chimica, Materiali e Ingegneria Chimica "Giulio Natta," Politecnico di Milano, 20133 Milano, Italy

[3]Istituto per i Polimeri, Compositi e Biomateriali (IPCB), Consiglio Nazionale delle Ricerche, 95126 Catania, Italy

[4]Istituto di Chimica dei Composti Organo Metallici (ICCOM), Consiglio Nazionale delle Ricerche, 56124 Pisa, Italy

[5]Dipartimento di Ingegneria Chimica, dei Materiali e della Produzione Industriale, Università di Napoli Federico II, 80125 Napoli, Italy

Correspondence to: N.D. Dintcheva (E-mail: nadka.dintcheva@unipa.it)

INTRODUCTION

Due to their unique and attractive mechanical, electrical, magnetic, optical, and thermal properties, carbon nanotubes (CNTs) have recently drawn the attention of both academic and industrial research for the formulation of innovative polymer based nanocomposites for demanding applications. Unfortunately CNTs are inclined to aggregate and/or agglomerate, which makes their uniform dispersion into a polymer matrix a difficult task.[1–3] A poor dispersion, which is often connected with an insufficient interfacial adhesion between the CNTs and polymer matrix, can nullify all the advantages of the nanometric size of this filler. Therefore, significant efforts have been directed towards developing methods to modify surface properties of CNTs and to improve the dispersion, such as an optimum physical blending, the *in situ* polymerization and also chemical functionalization.[4] This last can be carried out through (i) covalent linkage,[5] (ii) noncovalent supramolecular absorption,[6] (iii) defect functionalization,[7] and (iv) modification through click chemistry,[8] thus improving the compatibility of CNTs with polymeric materials and favoring a good degree of dispersion. Besides improving the dispersibility inside polymer matrices, the presence of specific organic groups/molecules anchored to the surface of the CNTs provides them new functionalities, enlarging the possible fields of application. Functionalized CNTs can be considered as nanovectors of the attached moiety thus allowing, once dispersed in a polymer matrix, to combine all

the structural advantages of this 1D nanofiller with the specific properties of the functional groups. Among the possible functionalizing agents, antioxidant (AO) molecules are receiving particular attention. The reason is that AO immobilization onto a nanosized substrate allows to elude issues related to the physical loss by volatilization, migration or water extraction.[9–12] In addition, the antioxidant activity can be optimized because the grafted AO is located at the polymer-particle interface, i.e., exactly where the local increase of the mechanical stresses experienced during compounding may generate oxidized species, thus promoting polymer degradation.

Recently we have successfully prepared antioxidant-functionalized CNTs (AO-*f*-CNTs) by covalent grafting of a hindered phenol derivative on the CNT sidewalls.[13] Aim of this article is investigating the ability of such multifunctional nanoparticles to actually improve the stability of a host polymer. Specifically, we selected ultra-high molecular weight polyethylene (UHMWPE), whose well-known thermo-oxidation mechanisms facilitate the assessment of the antioxidative activity of our AO-*f*-CNTs. The effectiveness of two alternative compounding methods is here compared. In particular, UHMWPE/CNTs samples were prepared by traditional melt mixing (MM) and through a hot compaction (HC) process able to improve the thermo-oxidative resistance of the material due to the milder processing conditions. The study is focused on the preparation of the composites and on the determination of the effective capability of the antioxidant functionalized CNTs to improve the thermo-oxidative behavior of the polymer matrix by investigating the thermo-oxidation resistance through rheological analyses and infrared spectroscopy.

EXPERIMENTAL

Materials

The UHMWPE is a commercial grade purchased by Sigma-Aldrich in the form of a white powder. Its main properties are: average molecular weight $M_w = 3$–6 MDa, softening point $T = 136$°C (Vicat, ASTM D 1525B), melting point $T_m = 138$°C, degree of crystallinity about 48.1% (estimated through DSC measurement considering a heat of fusion for perfectly crystalline polyethylene $\Delta H_f = 288.84$ J/g), and density $\rho = 0.94$ g/mL at 25°C. The average molecular weight was detected by means of intrinsic viscosity ($[\eta]$) measurements according to ASTM D4020-05 using a Lauda Pro-line PV15 viscometer. The UHMWPE was dissolved in decahydronaphtalene (reagent grade Sigma-Aldrich) at 150°C and maintained under magnetic stirring for 1 h. Based on elution time measurements, the value of $[\eta]$ was calculated using the Mark-Houwink relationship, and specifically, the Margolies equation:

$$M_v = 5.37 \times 10^4 \ [\eta]^{1.37}$$

Considering three independent measurements, the calculated average value of molecular weight is $M_v = 4.9 \times 10^6$ (g/mol).

Octadecyl-3-(3,5-di-*tert*-butyl-4-hydroxyphenyl)-propionate, a sterically hindered phenolic antioxidant (molecular weight 531 g/mol) commercialized by Ciba® Specialty Chemicals under the trade name of Irganox® 1076, was used as AO precursor. It was initially subjected to hydrolysis reaction to get the reactive antioxidant molecule (3-(3,5-di-*tert*-butyl-4-hydroxyphenyl) propanoic acid) to be covalently attached onto the CNT surface.

CNTs bearing antioxidant molecules grafted on the outer surface (AO-*f*-CNTs) and used in this work were produced starting from multiwalled CNTs containing ~1 wt % of covalently linked —OH groups (CNTs-OH) purchased by Cheap Tubes. The main features of the CNTs-OH are: outer diameter OD = 120–180 nm, inner diameter ID = 10–20 nm, length $L = 10$–20 μm, purity >95 wt %, ash <1.5 wt %, specific surface area SSA >60 m^2/g, and electrical conductivity EC $>10^{-2}$ S/cm.

The functionalization of CNTs-OH with the 3-(3,5-di-*tert*-butyl-4-hydroxyphenyl) propanoic acid was carried out in THF at room temperature using *N*,*N*′-dicyclohexylcarbodiimide (DCC) as a condensation reagent, as described in our previous article.[11] Bare multiwalled CNTs (purchased by Cheap Tubes. Outer diameter 120–180 nm, inner diameter 10–20 nm, length $L = 10$–20 μm, purity >95 wt %) were also used to produce reference samples.

All the chemicals used were reagent grades purchased by Sigma Aldrich and used as received.

Nanocomposite Preparation

UHMWPE-based nanocomposites containing 1 wt % of bare CNTs, CNTs-OH or AO-*f*-CNTs were prepared by hot compaction (HC) and melt mixing (MM). The HC process was performed using a hydraulic Carver press. Polymer and CNTs were manually mixed at room temperature to obtain a homogeneous black powder, which was loaded between the plates of the press and compressed at a pressure $P = 1500$ psi for 5 min at $T = 210$°C. The resulting thin films (thickness ~80 μm) were used for the subsequent analyses. The MM samples were prepared using a microcompounder (Minilab, Thermo-Haake), which consists of a co-rotating twin-screw extruder endowed with a feed-back channel. The extrusions were performed at $T = 210$°C and screw speed of 100 rpm. The residence time was 5 min. Then the extrudate was pelletized, and thin nanocomposite films were prepared using the Carver press. Pure UHMWPE and UHMWPE/AO (containing 0.1 wt % of free Irganox® 1076) thin films prepared by HC and MM were used as reference.

Characterization

Thermogravimetric analyses were carried out on the bare and functionalized CNTs by using an Exstar TG/DTA Seiko 7200 instrument. The tests were performed at a heating rate of 10°C/min from 30 to 750°C under nitrogen flow. The reported results are the average of three independent measurements on batches of ~5 mg. The standard deviation was ±0.3% for each investigated sample.

Applied Biosystems 4800 MALDI TOF/TOF™ Analyzer (Framingham, MA) mass spectrometer was used in this study to acquire MALDI spectra. The TOF/TOF instrument is equipped with a Nd:YAG laser (355 nm wavelength) of <500 ps pulse and 200 Hz repetition rate. MALDI-TOF/TOF-MS spectra were recorded in reflector positive ion mode. External calibration was performed by using angiotensin in MS/MS mode. Mass

accuracy was about 75 ppm. Preliminary qualitative experiments by using AO-f-CNTs and CNTs-OH as matrix were carried out.

The MALDI analyses were performed following the procedure reported in our previous work.[11]

Rheological tests were performed using a stress-controlled rheometer (mod. SR5 by Rheometric Scientific) in parallel plate geometry (plate diameter 25 mm). The complex viscosity (η^*) was measured performing frequency scans from $\omega = 10^{-1}$ to 10^2 rad/s at $T = 210$°C. The strain amplitude was $\gamma = 2\%$, which preliminary strain sweep experiments proved to be low enough to be in the linear viscoelastic regime.

Optical microscopy was performed using a Leica Microscope in reflection mode at a magnification of 20×. Images were acquired on the surface of the nanocomposite films.

Fourier transform-infrared spectroscopy (FT-IR) was carried out by using a Perkin Elmer FT-IR spectrometer (mod. Spectrum One). The spectra were collected on films subjected to a thermo-oxidation process carried out in oven at $T = 120$°C. The selected temperature is high enough to accelerate the degradation phenomena, and yet just below the onset of polymer melting (see Supporting Information, Figure S1).

FT-IR analyses were performed on films thermo-oxidized for different time. The spectra were collected by performing for each sample 16 scans between 4000 and 500 cm^{-1}. The progress of the degradation was quantified by referring to the carbonyl (CI) and hydroxyl (HI) indices: CI was calculated as the ratio between the integral of the carbonyl absorption region (1850–1600 cm^{-1}) and that of a reference peak at about 1370 cm^{-1} (1390–1330 cm^{-1}); HI refers to the hydroxyl absorption region (3570–3150 cm^{-1}), whose integral was normalized with respect to the integral of the peak at 1370 cm^{-1} (1390–1330 cm^{-1}). CI and HI are calculated as the difference between the areas of the carbonyl or hydroxyl peak (normalized by the reference peak) at the generic instant t and at the beginning of the test.

Extraction tests were performed with a Soxhlet extractor using *p*-xylene as solvent. Approximately 0.03 g of each sample were extracted by refluxing *p*-xylene for about 120 h.

RESULTS AND DISCUSSION

Preliminary Characterization of the AO-f-CNTs and UHMWPE-Based Nanocomposites

A reactive hindered phenol antioxidant molecule was successfully grafted onto the outer surface of the CNTs-OH [see Figure 1(a)]. The demonstration of the covalent nature of the bond formed between the AO and CNT surface in the functionalized AO-*f*-CNTs was the subject of a recent study by our group.[13] Specifically, the covalent linkage of the AO was inferred through MALDI-TOF mass spectrometry, see Figure 1(b). Since AO-*f*-CNTs cannot be directly used as MALDI analyte because of their high molecular weight, the functionalized nanoparticles were subjected to a thermal cleavage before the MALDI measurements. As a result, the CNTs and free AO obtained after hydrolysis of AO-*f*-CNTs represented the matrix and analyte, respectively. This innovative approach allowed for the univocal identification of AO and the demonstration of the covalent

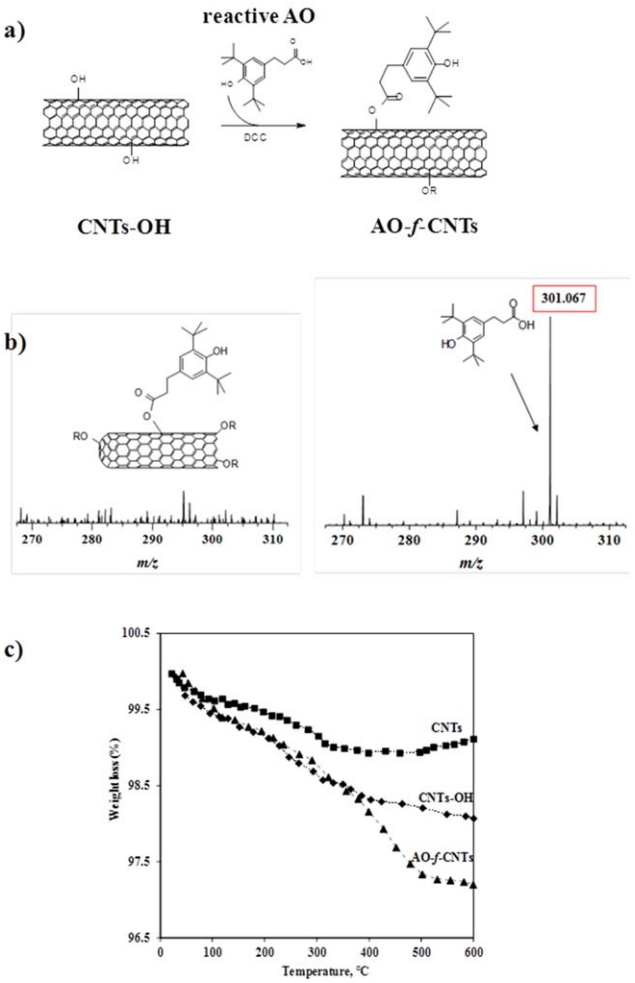

Figure 1. (a) Immobilization of the reactive AO molecule onto the CNT outer surface. (b) TGA curves of bare CNTs, CNTs-OH, and AO-*f*-CNTs. [Color figure can be viewed in the online issue, which is available at wileyonlinelibrary.com.]

linkage. Thermogravimetric analyses revealed an overall content of grafted AO moieties around 1 wt %, see Figure 1(c). The gradual weight loss related to the thermal decomposition of the AO groups takes place in the range 300 to 500°C, i.e. well above the temperature at which the nanocomposite thin films were prepared and characterized.

Rheology is particularly sensitive to the molecular architecture and can be profitably used to investigate the occurrence of the degradation phenomena in polymer matrices. Chain scission, branching, crosslinking, and other similar structural alterations bring about noticeable changes in the melt state behavior of macromolecular mediums. In addition, the rheological analysis of nanofilled polymers provides valuable information in terms of state of dispersion of the nanoparticles. Here, we performed linear viscoelastic measurements to infer the overall effect of the nanoparticles and of the degradation phenomena possibly occurring during the preparation of the samples. The complex viscosity curves of the neat UHMWPE, UHMWPE/AO, and the nanocomposites prepared by HC and MM processes are shown in Figure 2.

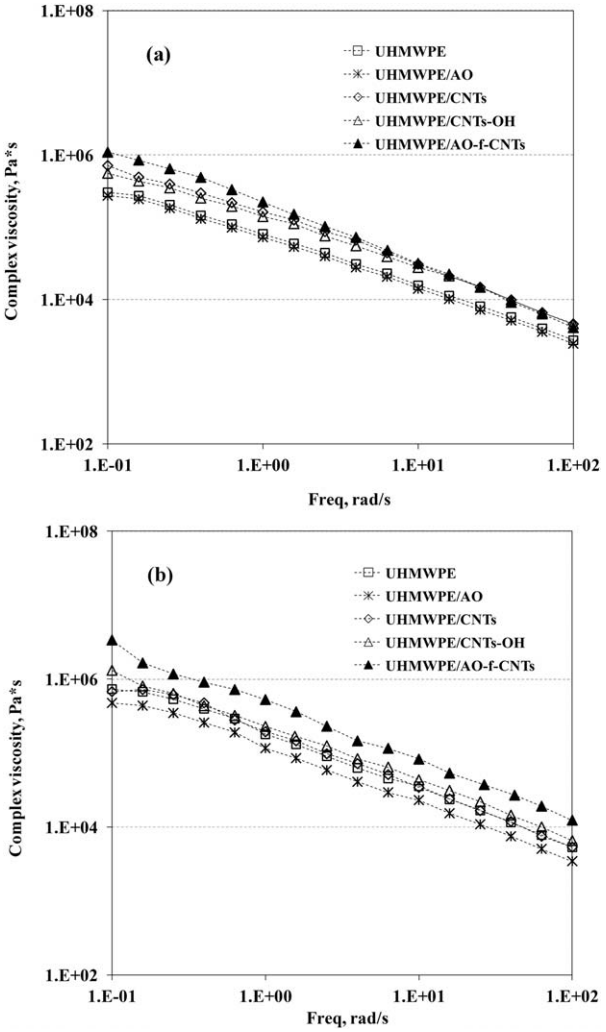

Figure 2. Complex viscosity of the UHMWPE-based nanocomposites prepared by HC (a) and MM (b). The complex viscosity curves of neat UHMWPE and UHMWPE/AO are reported for comparison.

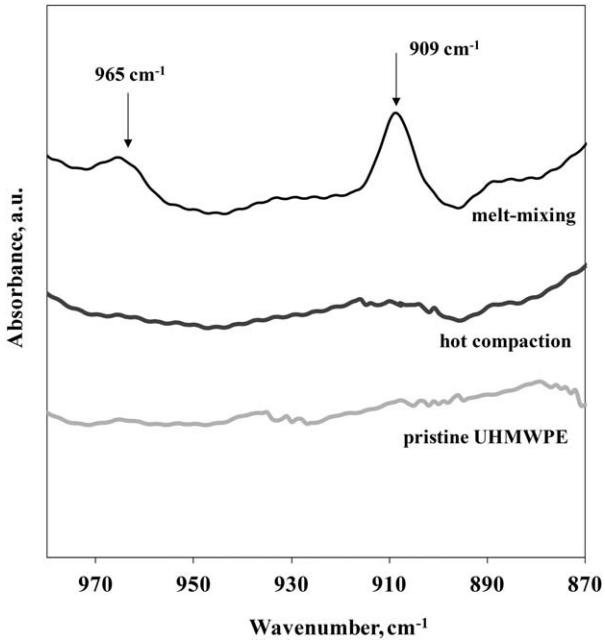

Figure 3. FT-IR spectra in the range 1000 to 870 cm^{-1} of MM and HC UHMWPE samples.

First we compared the effect of the processing routes on the neat UHMWPE. The complex viscosity of the UHMWPE treated by MM is ~50% higher than that of the polymer processed by HC in the whole range of investigated frequencies, meaning that the more intensive thermomechanical history experienced during extrusion likely promoted alterations in the molecular architecture of the polymer, thus affecting the entire relaxation spectrum. This is consistent with an increase of the average molecular weight due to branching, chain extension and/or crosslinking phenomena.[14] Solvent extraction tests actually revealed the presence of a fraction of about 5 wt % of insoluble polyethylene in the MM treated samples. The occurrence of crosslinking has been also confirmed by FT-IR analysis, see Figure 3. The spectrum of MM sample show two peaks at 965 and 909 cm^{-1}, which are due to trans-vinylene and terminal vinyl groups, respectively, both related to crosslinking formation.[15] Further proofs of the effects of a more intensive thermomechanical degradation undergone by the UHMWPE subjected to the MM process come from the FT-IR analysis addressed in the next section, which reveals the formation of oxidized species not detectable in the HC processed UHMWPE sample. The adding of free AO, which is large amount than the immobilized AO onto CNTs, does not affect the rheological behavior of UHMWPE processed by HC, see Figure 2(a), while, leads to a significant decrease of the viscosity values of UHMWPE processed by MM, see Figure 2(b). The latter can be understand considering the stabilizing action of free AO that is able to hinder the macromolecular structure alteration, such as crosslinking and/or branching, due to experienced thermomechanical degradation. In fact, the solvent extraction tests performed on UHMWPE/AO sample processed by MM show the presence of about 2 wt % of insoluble fraction, that is significantly reduced to the respect of pure UHMWPE processed by same route.

Concerning the effect of the nanoparticles, the CNTs addition caused a general increase of η^* in the HC processed samples. The effect being more pronounced in the presence of the AO-*f*-CNTs at low frequency that is the regime in which the melt state dynamics of large portions of material are probed. This phenomenon may be due to the arrangement of the functionalized AO-*f*-CNTs into branched structures, which span broad volumes of sample. Differently, the unmodified CNTs and the CNTs-OH caused a mere vertical shift of the η^* curve, without actually altering the relaxation spectrum. A similar effect can be explained by invoking the concept of the *shear stress equivalent inner shear rate*, proposed by Gleissle and Hochstein for suspensions of micron-sized particles.[16] In this case, the interstitial fluid between contiguous solid fillers experiences higher deformations than what externally imposed; as a result, the viscoelastic functions are fictitiously higher, but their frequency-dependence remains unaltered. Such an hydrodynamic effect anyway presumes an adequate dispersion of the filler, which seems to lack in the case of the MM processed samples

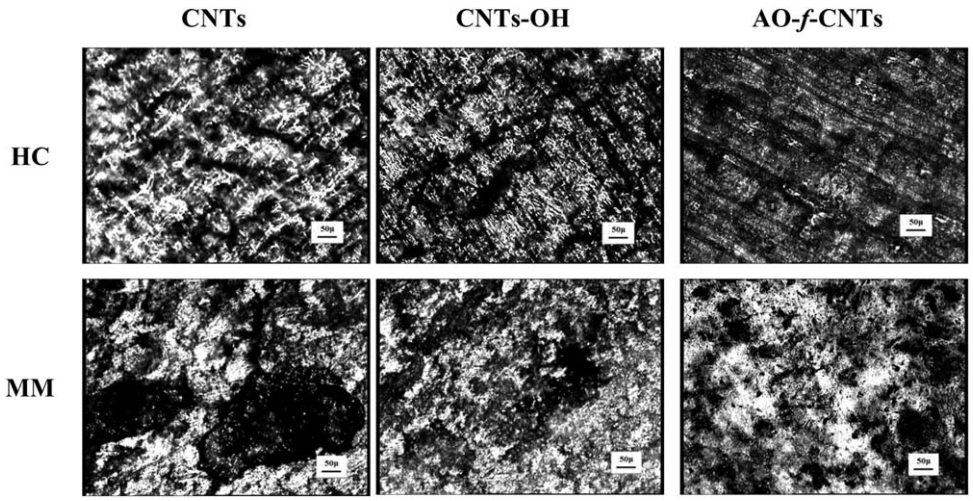

Figure 4. Representative optical micrographs of the surfaces of the UHMWPE-based nanocomposite films prepared by HC (top raw) and MM (bottom raw).

containing the unmodified CNTs and the CNTs-OH. In other words, the filler in these samples is likely dispersed too badly to generate appreciable rheological alterations. Some effect is noticed in the case of AO-*f*-CNTs, but unlike the corresponding HC treated sample, here the η^* curve is simply shifted above, suggesting a mere hydrodynamic effect of the agglomerated particles not assembled into big/branched structures.

The visual inspection of the nanocomposite films is in line with the indications emerged from the rheological analysis. Representative optical micrographs of the samples processed by HC and MM are shown in Figure 4. The CNTs appear as the dark phase.

The filler dispersion at the micron-scale in the HC processed samples appears finer than in the corresponding MM treated ones. In particular, venations and aggregates of few tens of microns in size penetrate the HC films irrespective of the CNT functionalization, while much bigger clusters are noticed in the MM processed samples. As discussed in the next section, the resulting agglomerates probably nullify most of the stabilizing effect of the AO molecules grafted onto the inner nanoparticles as previously,[10,11] which are, as a consequence, not exposed to the surrounding polymer.

Thermo-Oxidative Behavior of UHMWPE-Based Nanocomposites

The thermostabilizing action of the AO molecules grafted on CNTs and dispersed in the UHMWPE matrix is here investigated through the analysis of the evolution time of the FT-IR spectra of the composites during a thermo-oxidation process carried out in air at 120°C. The carbonyl (CI) and hydroxyl (HI) indices shown in Figure 5(a,b) are used to monitor the advance of the oxidation process. The CI indeed provides a inclusive measure of the intensity of the signals in the range 1850 to 1600 cm^{-1}, hence reflecting the formation of carboxylic acids (1713 cm^{-1}), ketones (1718 cm^{-1}), esters (1738 cm^{-1}), lactones (1786 cm^{-1}) and other oxygen-containing species, which form during oxidative degradation.[17,18] The HI reflects the formation of free and linked —OH groups deriving from the thermo-oxidation process. Indeed, as known, the thermo-oxidation mechanism for UHMWPE mainly concerns the peroxide and hydroperoxide formation and their later decomposition with formation of volatile products such as H_2O and, in lesser amounts, CO, CO_2, and H_2.[17] The growth of CI and HI hence provides information about the progress of the degradation phenomena.

First, the effect of the processing route on the stability of the unfilled UHMWPE is considered. The FT-IR spectra of the HC and MM samples in the range 1750 to 1600 cm^{-1} and 4000 to 3000 cm^{-1} are compared before the thermo-oxidation step [insets in Figure 5(a,b)]. The as-prepared MM processed sample shows two peaks at 1713 and 1637 cm^{-1} and well distinguishable shoulders in the range between 3400 and 3100 cm^{-1}, which reflect the presence of oxidized species not noticeable in HC treated samples. This is consistent with the rheological data, which indicated the occurrence of degradation of the neat UHMWPE in the course of the extrusion step. In fact, the applied mechanical stress on the polymer during melt mixing causes chain scission and subsequent formation of primary alkyl macroradicals, thus accelerating the degradation process.

Consider now the progress of oxidation phenomena in time. The carbonyl and hydroxyl indices at different thermo-oxidation times for all MM and HC processed samples are shown in Figure 5(a,b), respectively. Also the analysis of the oxidation kinetics indicates a detrimental effect of the MM route on the unfilled UHMWPE, which degrades more and faster than the sample processed by HC. An induction oxidation time can be readily identified for the HC samples, while the formation of oxygenated products for all the MM processed samples begins at the early stage of the thermo-oxidation. However, as a first approximation we can define a conventional induction time t_i for all the samples as the time needed for CI reaches the value of 5 and HI reaches 2 (see Figure 5). The estimated t_i values are summarized in Table I.

Regarding the effect of the unmodified CNTs, it can be noticed that the CI and HI of both the HC and MM prepared

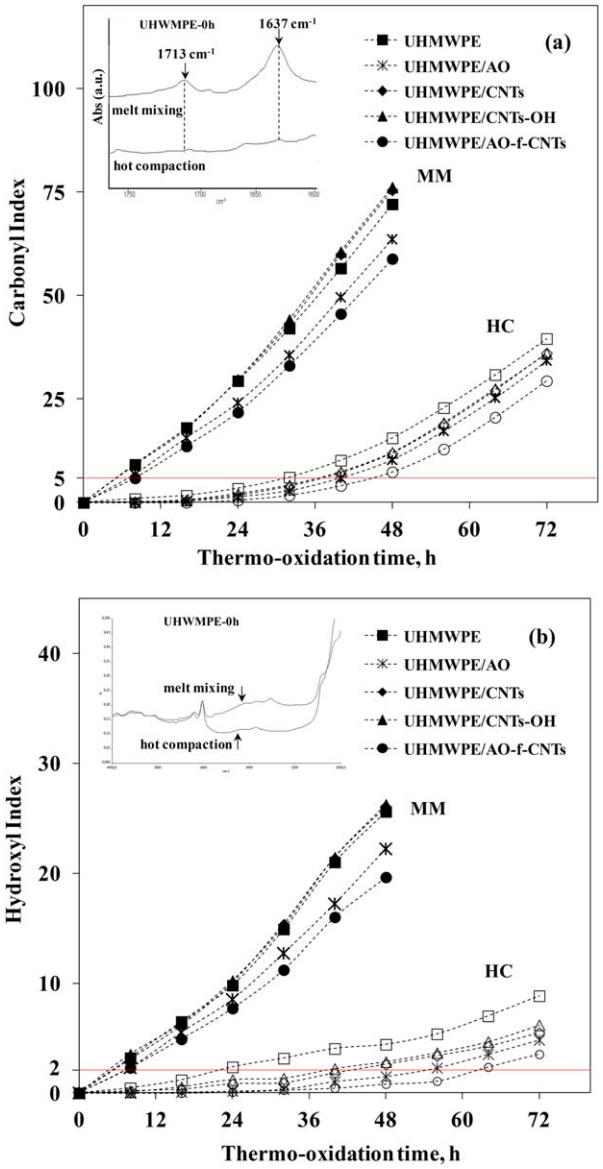

Figure 5. Carbonyl index (a) and hydroxyl index (b) as a function of the thermo-oxidation time for UHMWPE (squares), UHMWPE/AO (star) UHMWPE/CNTs (diamonds), UHMWPE/CNTs-OH (triangles) and UHMWPE/AO-*f*-CNTs (circles) processed by MM (full symbols) and HC (empty symbols). The inserts show the FT-IR spectra in the range 1750 to 1600 cm^{-1} (a) and 4000 to 3000 cm^{-1} (b) for the unfilled UHMWPE processed by MM and HC before thermo-oxidation. [Color figure can be viewed in the online issue, which is available at wileyonlinelibrary.com.]

nanocomposites essentially follow the same trends as the corresponding unfilled matrices: the former degrades less and more slowly than the latter. It is interesting to observe that, despite a documented CNTs radical scavenger activity,[19–21] the MM sample reaches values of CI and HI slightly higher than the unfilled matrix over long thermo-oxidation times. On the contrary, the bare CNTs seem to exert their weak antioxidant feature in the HC processed sample, whose long-term CI and HI values are a bit lower than those of the pure UHMWPE. As known, isolated aggregates of CNTs can act as thermal energy absorbing sites, thus inducing a local increase of the temperature. The latter

Table I. Values of the Thermo-Oxidation Induction Time

	t_i at CI = 5 (h)		t_i at HI = 2 (h)	
	HC	MM	HC	MM
UHMWPE	30.5	4.7	21.9	4.5
UHMWPE/AO	39	6.6	54.5	7.2
UHMWPE/CNTs	36.2	4.7	42.5	5.3
UHMWPE/CNTs-OH	35.8	4.7	39.1	5.2
UHMWPE/AO-*f*-CNTs	44.1	7.6	62.6	7.3

leads to an acceleration of the oxidation phenomena in CNTs additivated nanocomposites.[22] In our case, such an effect specifically concerns the MM treated samples, according to the morphological observation discussed before.

The presence of OH functional groups on the CNTs-OH surface has no appreciable effects. Indeed, the UHMWPE/CNTs-OH samples shows the same degradation kinetics as their reference UHMWPE/CNTs samples.

Let us now consider the samples AO-containing samples. As expected, the presence of 0.1 wt % of free AO in UHMWPE/AO samples produced by both processing routes slow down the thermo-oxidation phenomena, due to the well known stabilizing action of the used antioxidant.

The effect is even better in the samples containing the AO-*f*-CNTs. In percentage terms, the effect is more prominent for the HC treated sample, which could benefit from the better dispersion of the filler, emerged from the rheological and morphological analyses. In order to be effective, the antioxidant molecules grafted on the outer surface of the CNTs have to be exposed toward the polymer. As a consequence, the more extended polymer-filler interface of the HC sample could optimize the stabilizing action of the AO, while the aggregated feature of the AO-*f*-CNTs in the MM processed sample shields the effect of a considerable fraction of AO. It is important to underline that the effect of stabilization here observed was achieved by adding a very low amount of stabilizing molecule. Indeed, in our previous work[11] we estimated that the percentage of AO grafted groups on CNTs is about 1 wt %. This means that only ~0.01 wt % of AO molecules were present in the sample UHMWPE/AO-*f*-CNTs, i.e., a value 10 times lower than the amount of free AO added to the unfilled polymer to get a comparable improvement of the thermo-oxidation resistance. Such a noticeable effect of stabilization of the matrix was probably achieved thanks to the immobilization of the AO moieties on the CNTs sidewalls combined with an optimization of the dispersion. In this way the aggregation between the AO molecules is controlled (considering also the low amount), the migration and volatilization are avoided and, the AO action is much more effective than in case of simply mixing with the unfilled matrix.[10–12]

To explain the stabilization action of AO-*f*-CNTs, a possible antioxidant mechanism is proposed (see Figure 6). The assessed effectiveness of AO-*f*-CNTs can be ascribed to the combined action of the grafted hindered phenol moieties and of the CNTs, probably acting as radical scavengers.[23] The hindered

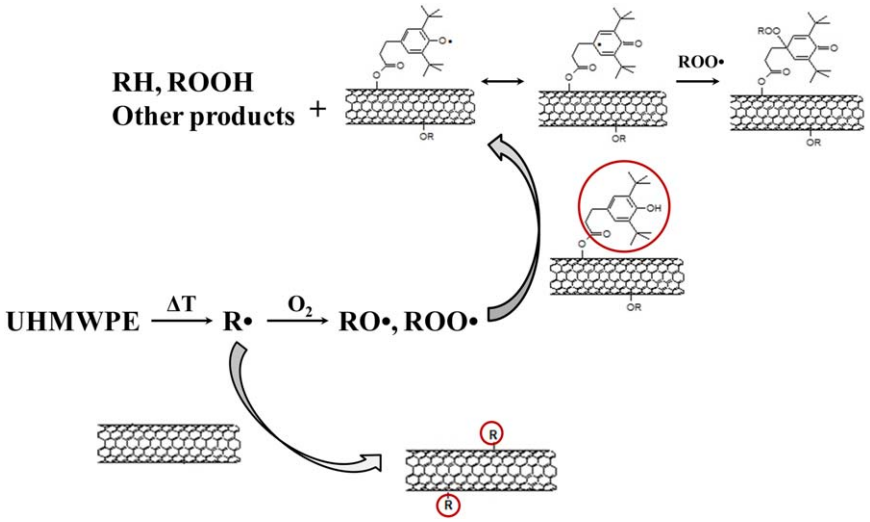

Figure 6. Schematic representation of antioxidant mechanism of AO-*f*-CNTs. [Color figure can be viewed in the online issue, which is available at wileyonlinelibrary.com.]

phenol moieties, being directly exposed toward the polymeric phase, likely act as a chain-breaking hydrogen donor, being able to convert the peroxyl radicals formed during the thermo-oxidative degradation into ROOH species.[24] In addition, as reported in literature, the CNTs act as antioxidants intervening in the first stage of the polyolefin thermo-oxidation and preventing the formation of oxygen-containing radicals.[25] Moreover, the radical scavenging activity of CNTs can be also ascribed to their acceptor-like electronic properties, caused by lattice defect onto their surface.[21,24–27]

Finally, we observe that, besides demonstrating the effectiveness of our approach, the improved stability of the UHMWPE/AO-*f*-CNTs samples proves that CNTs can be profitably used as a substrate on which grafting molecules carrying a specific functionality. Dispersing functionalized CNTs in a polymer matrix instead of the free functional molecules could limit the issues related to their migration during both the process and lifecycle of the product. Here we dealt with antioxidant molecules, but it is important to note that the approach is quite general, and the nature of both functional molecules and nanoparticles can be properly selected to design polymer materials for demanding applications.

CONCLUSIONS

Multiwalled carbon nanotubes (CNTs) functionalized with hindered phenol moieties (AO-*f*-CNTs) were were dispersed in ultra-high molecular weight polyethylene via two different compounding methods, namely melt mixing (MM) and hot compaction (HC). The resulting nanocomposites were characterized by means of rheological and morphological analyses, and their resistance to thermo-oxidation was assessed through spectroscopic techniques. The compounding procedure influenced the stability of the materials. In particular, the MM route resulted to have a detrimental effect even on the neat polymer, which begins to degrade already in the course of the process due to the intensive thermomechanical stresses involved in the extrusion. Similarly, the MM treated samples containing unfunctionalized CNTs exhibited accelerated degradation with respect to the HC processed samples. The high temperature reached during extrusion due to viscous dissipation accelerates the thermo-oxidation, nullifying the weak stabilizing action of CNTs instead noticed in the HC treated sample and ascribed to the documented radical scavenger activity of this kind of filler. The AO-*f*-CNTs clearly exerted thermo-stabilizing action in both the MM and HC processed sample, but the effect in the latter was more important. Based on the results of rheological and morphological analyses, the greater stability of the HC sample was ascribed to a better filler dispersion, which maximizes the extent of polymer-particle interface and, hence, optimizes the stabilizing action of the AO. A possible antioxidant mechanism is proposed to account for the stabilizing action exerted by the AO-*f*-CNTs. Overall, our results prove that CNTs can be profitably used as carriers of small molecules with specific functionality to be dispersed in a host polymer matrix, thus likely limiting the issues related to the migration of the additives during both the process and lifecycle of the product.

ACKNOWLEDGMENTS

This work was supported by the FIRB 2010—Futuro in ricerca project (No. RBFR10DCS7) funded by the Italian Ministry of University and Research (MIUR).

REFERENCES

1. Spitalsky, Z.; Tasis, D.; Papagelis, K; Galiotis, C. *Prog. Polym. Sci.* **2010**, *35*, 357.
2. Coleman, J. N.; Khan, U.; Blau, W. J.; Gun'ko, Y. K. *Carbon* **2006**, *44*, 1624.
3. Dintcheva, N. Tz.; Arrigo, R.; Nasillo, G.; Caponetti, E.; La Mantia, F. P. *Macromol. Mater. Eng.* **2011**, *296*, 645.
4. Xie, X. L.; Mai, Y. W; Zhou, X. P. *Mater. Sci. Eng. R* **2005**, *49*, 89.
5. Yang, M.; Gao, Y.; Li, H; Adronov, A. *Carbon* **2007**, *45*, 2327.

6. Nativ-Roth, E.; Shvartzman-Cohen, R.; Bounioux, C.; Florent, M.; Zhang, D.; Szleifer, I.; Yerushalmi-Rozenet, R. *Macromolecules* **2007**, *40*, 3676.
7. Mawhinney, D. B.; Naumenko, V.; Kuznetsova, A.; Yates, J. T.; Liu, J.; Smalley, R. E. *Chem. Phys. Lett.* **2000**, *324*, 213.
8. Campidelli, S.; Ballesteros, B.; Filoramo, A.; Dıaz, D. D.; Torre, G.; Torres, T.; Aminur Rahman, G. M.; Ehli, C.; Kiessling, D.; Werner, F.; Sgobba, V.; Guldi, D. M.; Cioffi, C.; Prato, M.; Bourgoin, J. P. *J. Am. Chem. Soc.* **2008**, *130*, 11503.
9. Gao, X.; Hu, G.; Qian, Z.; Ding, Y.; Zhang, S.; Wang, D.; Yang, M. *Polymer* **2007**, *48*, 7309.
10. Zhong, B.; Shi, O.; Jia, Z.; Luo, Y.; Chen, Y.; Jia, D. *Polym. Degrad. Stab.* **2014**, *110*, 260.
11. Gao, X.; Meng, X.; Wang, H.; Wen, B.; Ding, Y.; Zhang, S.; Yang, M. *Polym. Degrad. Stab.* **2008**, *93*, 1467.
12. Chen, J.; Yang, M. S.; Zhang, S. M. *Compos A* **2011**, *42*, 471.
13. Carroccio, S. C.; Curcuruto, G.; Dintcheva, N. Tz.; Gambarotti, C.; Coiai, S.; Filippone, G. *Rapid. Commun. Mass. Spectrom.* **2013**, *27*, 1359.
14. Tàtraalijai, D.; Földes, E.; Pukánszky, B. *Polym. Degrad. Stab.* **2014**, *102*, 41.
15. Bracco, P.; Brunella, V.; Luda, M. P.; Zanetti, M.; Costa, L. *Polymer* **2005**, *46*, 10648.
16. Gleissle, W.; Hochstein, B. *J. Rheol.* **2003**, *47*, 897.
17. Costa, L.; Luda, M. P.; Trossarelli, L. *Polym. Degrad. Stab.* **1997**, *58*, 41.
18. Bertoldo, M.; Bronco, S.; Cappelli, C.; Gragnoli, T.; Andreotti, L. *J. Phys. Chem. B* **2003**, *107*, 11880.
19. Martinez-Morlanes, M. J.; Castell, P.; Alonso, P. J.; Martinez, M. T.; Puertolas, J. A. *Carbon* **2012**, *50*, 2442.
20. Dintcheva, N. Tz.; La Mantia, F. P.; Malatesta, V. *Polym. Degrad. Stab.* **2009**, *94*, 162.
21. Watts, P. C. P.; Fearon, P. K.; Hsu, W. K.; Billingham, N. C.; Kroto, H. W.; Walton, D. R. M. *J. Mater. Chem.* **2003**, *13*, 491.
22. Morlat-Therias, S.; Fanton, E.; Gardette, J. L.; Peeterbroeck, S.; Alexandre, M.; Dubois, P. *Polym. Degrad. Stab.* **2007**, *92*, 1873.
23. Galano, A. *J. Phys. Chem. C* **2008**, *112*, 8922.
24. Shi, X.; Wang, J.; Jiang, B.; Yang, Y. *Polymer* **2013**, *54*, 1167.
25. Shi, X.; Jiang, B.; Wang, J.; Yang, Y. *Carbon* **2012**, *50*, 1005.
26. Dintcheva, N. Tz.; Arrigo, R.; Gambarotti, C.; Carroccio, S.; Filippone, G.; Cicogna, F.; Guenzi, M. *Carbon* **2014**, *74*, 14.
27. Arrigo, R.; Dintcheva, N. Tz.; Guenzi, M.; Gambarotti, C.; Filippone, G.; Coiai, S.; Carroccio, S. *Polym. Degrad. Stab.* **2015**, *115*, 129.